ADVANCED ENGINEERING MATERIALS

DOI: 10.1002/adem.201100019

Strength and Ductility of Bi-Modal Cu**

By *Yonghao Zhao,* Troy Topping, Ying Li* and *Enrique J. Lavernia*

Engineering a microstructure with multiple length scales has been proposed as a strategy to enhance the plasticity of nanostructured materials which otherwise lack extensive dislocation activity, and therefore low ductility. To that effect, various research groups have implemented this concept by promoting the formation of so called bi-modal microstructures (e.g., consisting of a mixture of ultrafine and micro-grains) with balanced combinations of strength and ductility. Despite encouraging results, fundamental, information on important questions remained unanswered. For example, what is the relationship between the volume fraction of the coarse grained phase and the overall ductility? What is the influence of size of the coarse grained phase, and how does its distribution influence ductility? To provide insight into these, and other related questions, in this work, we prepared bimodal Cu with homogeneous distribution of different-volume-fraction micro-grains via isothermal recrystallization of an ultrafine grained Cu matrix at 200 °C. Analysis of the tensile results and microstructural characterization suggest that both strength and ductility of the bi-modal Cu follows the rule-of-mixtures, with interesting results related to volume fraction. Our work provides a pathway for optimizing the mechanical properties of multiscale materials.

Bulk ultrafine grained (UFG) materials possess high strength but low ductility, which has evolved into a seemingly insurmountable obstacle for widespread technological applications of these new materials.[1] Recently, various strategies have been developed for improving the poor ductility of bulk UFG materials,[2] among which, introducing a bi- or multi-modal grain size distribution has been found to be broadly applicable to many material systems.[3–6] These bi-modal or multi-modal materials usually have a wide grain size distribution ranging from the UFG (i.e., <500 nm) to the coarse-grained (CG, >1 μm) regions,[7] and they can be prepared by either abnormal grain growth via annealing-induced secondary recrystallization of UFG materials[5,8] or via the consolidation of mixtures of multi-scale size particles.[4,6] With the former technique, it is difficult to quantitatively control the multi-scale grain structures by controlling recrystallized nucleation sites and growth kinetics due to the highly unstable high-energy states of UFG microstructures.[8,9] The latter method allows for more accurate control of the multi-scale grain structures by simply controlling the mixing ratio of different-size particles. However, the processing artifacts, such as nanopores and incomplete bonding that are sometimes introduced by the consolidation process, may obscure the intrinsic mechanical property-structure relationships.[4,10] The UFG grains in bi-modal materials are known to promote a high strength by limiting dislocation movement, whereas the micron-sized grains occupy a larger proportion of the microstructure on a volumetric basis, thus increasing their effect on the behavior of the aggregate, such as ductility, by suppressing crack growth and facilitating plastic deformation.[4]

Although a large amount of published work has qualitatively verified that the introduction of multi-scale grain structures can indeed improve the poor ductility of UFG materials,[11–22] this approach represents in fact, a compromise strategy: i.e., to achieve ductility by sacrificing strength. The question is what is the extent of such a compromise? Or can one predict the behavior of multi-scale materials using simple weighted averages of the strength and ductility of UFG and CG components, i.e., following the rule-of-mixtures?[23] Interestingly, the published literature reveals two principal, and contradictory, trends: both positive (i.e., improved) and negative (i.e., diminished) deviations from the rule-of-mixtures have been reported. As an example of the former case (e.g., positive deviation), Wang *et al.*[5] reported that an introduction of 25% volume fraction of CGs into an UFG Cu matrix resulted in a 30% uniform elongation and a comparable

[*] *Dr. Y. H. Zhao, T. Topping, Y. Li, Prof. E. J. Lavernia*
Department of Chemical Engineering and Materials Science
University of California at Davis, CA 95616, (USA)
E-mail: yhzhao@ucdavis.edu

[**] *The support from the Office of Naval Research (N00014-08-1-0405) is greatly appreciated. Prof. Ruslan Z. Valiev is acknowledged for providing UFG Cu samples.*

elongation to failure (65%) with that of the CG Cu counterpart (70%), while the yield strength was still maintained about five to six times higher than that of the CG Cu. This, in fact, represents an excellent compromise, because the simultaneous high strength and high ductility, especially the very large uniform elongation, results in a notable gain in static toughness (the area under the stress–strain curve). Similar results were reported by Jin and Lloyd[12] with a 5754 Al–3.1Mg–0.3Mn–0.2Fe–0.1Si alloy (wt%). In addition to experimental results, a positive deviation from the rule-of-mixtures has also been predicted on the basis of numerical analysis by Sevillano and Aldazabal[24] who used one-dimensional cellular automaton model to simulate the elastic and plastic deformation of bi-modal materials. The model takes into account inter-grain orientations and inter-/intra-grain dislocation densities and internal stress heterogeneities. By randomly mixing different fractions of the unimodal UFG structure (130 nm) and the unimodal CG structure (25 μm), the authors found that the uniform elongation increases first rapidly and then slowly with decreasing volume fraction of UFG matrix, which results in a marked improvement in uniform elongation and the overall ductility of bimodal materials relative to those corresponding to unimodal materials possessing the same strength. As a result, a significant gain in toughness is attained, and the ductility of bimodal polycrystal exceeds the prediction of the rule-of-mixtures. In contrast, a negative deviation from the rule-of-mixtures was observed during thermal annealing a nanocrystalline Cu prepared by dynamic plastic deformation (DPD) at liquid nitrogen temperature.[8] In this study, with increasing volume fraction of CGs, the strength decreased, and the ductility increased gradually to reach the value of the CG Cu (42%), a remarkable increase in uniform elongation occurred only when the volume fraction of macro-grains exceeded 90 vol%. Similar results were also reported by Fan *et al*. in bi-modal 5083 Al–Mg alloy,[13] Fe,[14] Ni,[17] Cu.[18–20]

To rationalize the mechanisms that may be responsible for the above contradictory trends, it is important to consider differences in the microstructure, such as the spatial distribution of the UFG and CG grains, or possibly any grain size differences between the UFG matrix and CGs. Moreover, in the case of a multi-scale microstructure, the grain size distribution histogram is, in fact, not sufficient to completely describe the microstructures. Therefore, systematic investigations are necessary to quantitatively reveal the mechanical properties and microstructure relationships, first in the case of bi-modal materials, and ultimately, for multiscale microstructures. In the present study, we propose the approach of systematically controlling the distribution of Cu UFG and macro-grains to provide insight into the dependence of strength and uniform elongation on the overall microstructure architecture.

Experimental

High-purity UFG copper (99.99%) square bars (20 mm × 20 mm) were prepared by equal-channel-angular pressing (ECAP) at ambient temperature for 16 passes by route Bc in which the sample was rotated by 90° in the same sense between each pass in the procedure.[25] The ECAP die has an L-shape channel with an intersecting channel angle of 90° and an outerarc angle of 45° which imposes an effective strain of approximately one per ECAP pass. The 16 processing passes resulted in homogeneous UFG structure matrix for the subsequent nucleation and abnormal grain growth.

The as-ECAPed UFG Cu was then annealed at 200 °C in silicone oil for different durations (5, 20, 40, 90, and 480 min) to form homogeneous bi-modal structures with different volume fractions of recrystallized micro-grains. An oil-bath was used for annealing in order to minimize local fluctuations in temperature. To obtain a CG Cu reference sample, part of the UFG Cu was annealed at 500 °C in Ar protective atmosphere for 2 h.

Flat dog-bone tensile specimens with gauge dimensions of 10 mm × 1 mm × 2 mm were sectioned by electrical discharge machining (EDM) from the central regions of the UFG Cu square bars with a gauge axis parallel to the extrusion direction and a gauge surface parallel to top plane of the extrusion bar. Uniaxial tensile tests were performed at room temperature on an Instron 8801 universal testing machine (UTM) with an initial quasi-static strain rate of 10^{-3} s^{-1}. The strain was measured by using a standard non-contacting video extensometer with a 100 mm field-of-view lens.

The grip sections of the tensile specimens were examined using transmission electron microscopy (TEM) at a Philips CM12 microscope operated at 100 kV and electron back-scattered diffraction (EBSD) at a TSL OIM system on a Philips XL30 FEG SEM with step sizes of 50–100 nm. TEM specimens were prepared by first mechanically grinding the samples to a thickness of about 50–70 μm, then dimpling to a thickness of about 10 μm, and finally ion-milling to a thickness of electron transparency using a Gatan Precision Ion Milling System with an Ar+ accelerating voltage of 4 kV and a temperature below 35 °C. The EBSD samples were first polished using a diamond lapping film (particle diameter 1 μm) and then electro-polished in a solution of 66% H_3PO_4 and 34% H_2O at 2 V.

Results and Discussion

Mechanical Properties

The engineering stress–strain curves of as-ECAP'ed UFG and the annealed bi-modal Cu samples are shown in Figure 1(a). It is apparent that the as-ECAP'ed Cu sample has a dominant post-necking elongation, i.e., necking instability occurred shortly after yielding. This geometrical instability is typical phenomenon of UFG metals processed by severe plastic deformation due to lack of strain hardening and dislocation accumulation capability. As listed in Table 1, the as-ECAP'ed Cu sample has a 0.2% yield strength of 370 MPa, ultimate tensile strength of 410 MPa, an uniform elongation of 2% and an elongation to failure of 16%.

Annealing gradually decreased the strength of the Cu sample by enhancing gradual increases in strain hardening

ADVANCED ENGINEERING MATERIALS

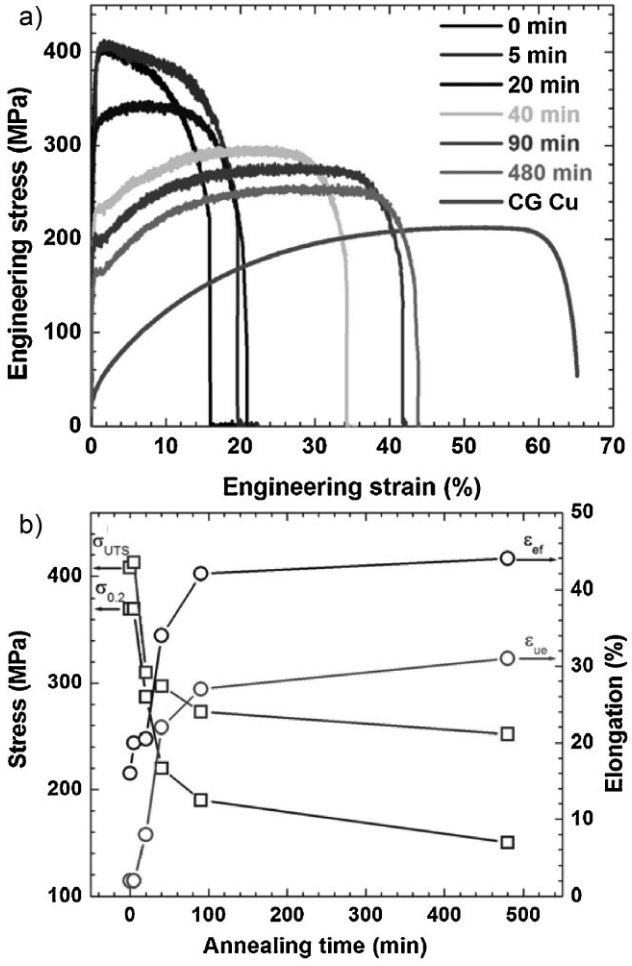

Fig. 1. (a) Tensile engineering stress–strain curves of the annealed bi-modal Cu samples (annealing time was indicated) at a strain rate of 10^{-3} s^{-1}. (b) Variations of yield strength $\sigma_{0.2}$, ultimate tensile strength σ_{UTS}, uniform elongation ε_{ue} and elongation to failure ε_{ef} of the annealed bi-modal Cu versus annealing time.

Table 1. A list of yield strength $\sigma_{0.2}$, ultimate tensile strength σ_{UTS}, uniform elongation ε_{ue}, elongation to failure ε_{ef}, and volume fraction of recrystallized region X_V of the annealed bi-modal Cu.

Annealing time [min]	$\sigma_{0.2}$ [MPa]	σ_{UTS} [MPa]	ε_{ue} [%]	ε_{ef} [%]	X_V [%]
0	370	410	2	16	0
5	370	413	2	20	8
20	310	342	9	20.5	30
40	220	297	18	34	65
90	190	273	21	42	
480	150	252	26	44	100
CG	30	210	55	65	

and ductility [Fig. 1(a)]. Figure 1(b) shows the variations of yield strength $\sigma_{0.2}$, ultimate tensile strength σ_{UTS}, uniform elongation ε_{ue}, and elongation to failure ε_{ef} of the annealed bimodal Cu versus annealing time. With increasing annealing time from 0 to 480 min, the yield strength decreases gradually from 370 to 150 MPa and the elongation to failure increases

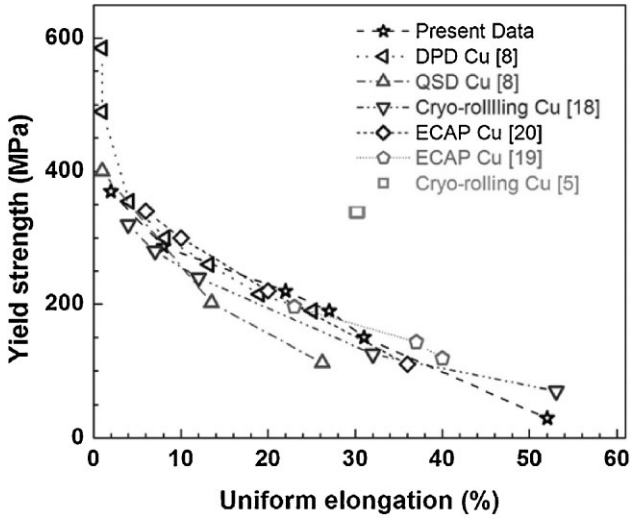

Fig. 2. Yield strength versus uniform elongation of the bi-modal Cu prepared by DPD and QSD,[8] cryo-rolling,[5,18] ECAP,[19,20] and subsequent annealing.

from 16 to 44% gradually. The CG Cu has a yield strength of 30 MPa, and a ductility of 65%.

Figure 2 illustrates yield strength against uniform elongation of the bi-modal Cu prepared by DPD and quasi-static deformation (QSD),[8] cryo-rolling,[5,18] ECAP,[19,20] and subsequent annealing. Here, we compare the uniform elongation values, but not the elongation to failure, from different groups because our recent studies indicate that the former is not affected by tensile specimen size or geometry.[26,27] Except the data from Wang *et al.*,[5] annealing enhances the uniform elongation with a concomitant decrease in yield strength. That is, the $\sigma_{0.2}$–ε_{ue} of the Cu samples exhibit approximately linear relationships: $\sigma_{0.2}$ and ε_{ue} are inversely proportional to each other, i.e., lowering strength increases ductility, and vice versa.

Microstructures

Figure 3 presents typical bright-field TEM images and the corresponding selected area diffraction (SAD) patterns (taken from an area with a diameter of 5.4 μm) of the as-ECAP'ed and annealed Cu samples (5, 20, 40, and 480 min). The as-ECAP'ed Cu sample is composed of equiaxed grains with sizes ranging from about 100 to 700 nm and an average size of about 300 nm. Moreover, two types of boundaries were observed: sharp and straight equilibrium boundaries (as indicated by white arrows) and wavy distorted boundaries (indicated by black arrows in the Fig. 3). The sharp equilibrium boundaries may have originated from relaxation and recovery during the ECAP process due to the fact that the grains neighboring these boundaries are clean and free of dislocations, and these represent ≈20 vol% of the overall boundaries. The wavy distorted boundaries are mainly subgrain (dislocation cell) boundaries with low-angle misorientation. The geometrical arrangement, namely wavy distorted boundaries, suggests that these may be non-equilibrium boundaries.[28] Non-equilibrium boundaries contain a high density of

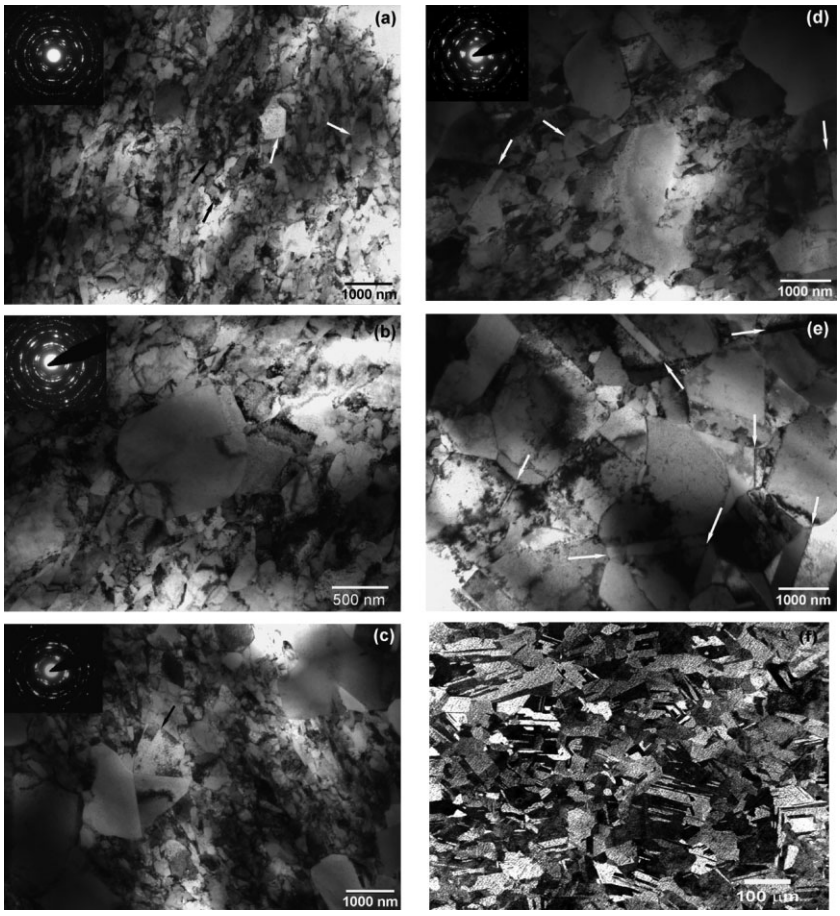

Fig. 3. Typical bright-field TEM images and the corresponding SAD patterns (taken from an area with a diameter of 5.4 μm) of the as-ECAPed (a) and annealed bi-modal Cu with annealing time of 5 (b), 20 (c), 40 (d), and 480 min (e). The annealing twins are pointed by white arrows in Figure 2(c–e). Sharp and straight equilibrium boundaries and wavy distorted subgrain (dislocation cell) boundaries are pointed by white and black arrows in Figure 2(a), respectively. The innermost ring in SAD patterns might originate from CuO due to oxidation. (f) Optical metallography of the CG Cu reference sample with an average grain size of 50 μm and high-density annealing twins.

extrinsic dislocations, which are not needed to accommodate the misorientation across the grain boundary.[28] The above microstructural characteristics during the ECAP process are consistent with the results reported in the literature.[29]

After annealing for 5 min, as shown in Figure 3(b), recrystallized micro-grains with a size of ≈1 μm appeared and were uniformly distributed among the UFG Cu matrix. Statistical analyses of large TEM observation areas indicate that the volume fraction of the recrystallized micro-grains, X_V, is ≈8%. Annealing for 20 min promoted the formation of ≈30% volume fraction of recrystallized micro-grains with sizes ranging from 1 to 3 μm and low density of annealing twins decorated within the micro-grains [marked by black arrows in Figure 3(c)]. The micro-grains are uniformly distributed within UFG Cu matrix, although 2 or 3 recrystallized micro-grains assembles are occasionally observed. When the UFG Cu sample was annealed for 40 min, the recrystallized coarse grains dominated the sample with a volume fraction of about 65%. As shown in Figure 3(d), the recrystallized macro grains are inter-connected so that the UFG regions are separated into isolated regions. The recrystallization process was complete following the 480 min anneal, manifested by the 100% volume fraction of the recrystallized 1–3 μm grains, as shown in Figure 3(e). Annealing twins were frequently observed, as highlighted by white arrows in Figure 3(d,e). Optical metallography indicates that the grain size of the CG Cu reference sample is about 50 μm, as shown in Figure 3(f). A high density of annealing twins, with spacing ranging from several micrometers to tens of micrometers, was observed within the coarse grains.

To further confirm the microstructures of the bimodal Cu, we performed EBSD analysis. Figure 4 shows the typical EBSD results for the bimodal Cu annealed for 40 min. From Figure 4(a), it is apparent that the recrystallized micro-grains (1–3 μm) are dominant and uniformly distributed within the UFG matrix. Quantitative calculation indicates that the volume fraction of the recrystallized macro-grains is about 70% which is in agreement with the TEM results. Figure 4(b) shows (001), (101), and (111) pole figures in stereographic projection of the bi-modal Cu which exhibits ill-defined textures suggestive of a small sampling from a random distribution. Random textures would be expected from the annealing processing.

Recrystallization Kinetics

The recrystallization kinetics are shown in Figure 5, after incubation X_V increased linearly and saturated to 100%. On the basis of the well-known JMAK equation:[30]

$$X_V = 1 - \exp(-Bt^n) \quad (1)$$

where t is the annealing time, and n is Avrami exponent, the n value calculated from the present results is about 1.3, which is smaller than 4 for an assumption of constant rates of nucleation and growth and 3 for an assumption of site saturated nucleation. Inspection of the scientific literature shows that n values on the order of 1 have been reported in Al,[31] Cu,[32] and Fe.[33] These results suggest that perhaps the JMAK analysis contains too many limiting assumptions to accurately describe the complex recrystallization process. For example, the specific microstructural changes that occur during recrystallization require other parameters, in addition to the fraction of material transformed X_V. Vandermeer and Gordon.[34] improved the JMAK approach using microstructural path methodology in which more realistic and more complex geometric models are employed by using additional microstructural parameters.

ADVANCED ENGINEERING MATERIALS

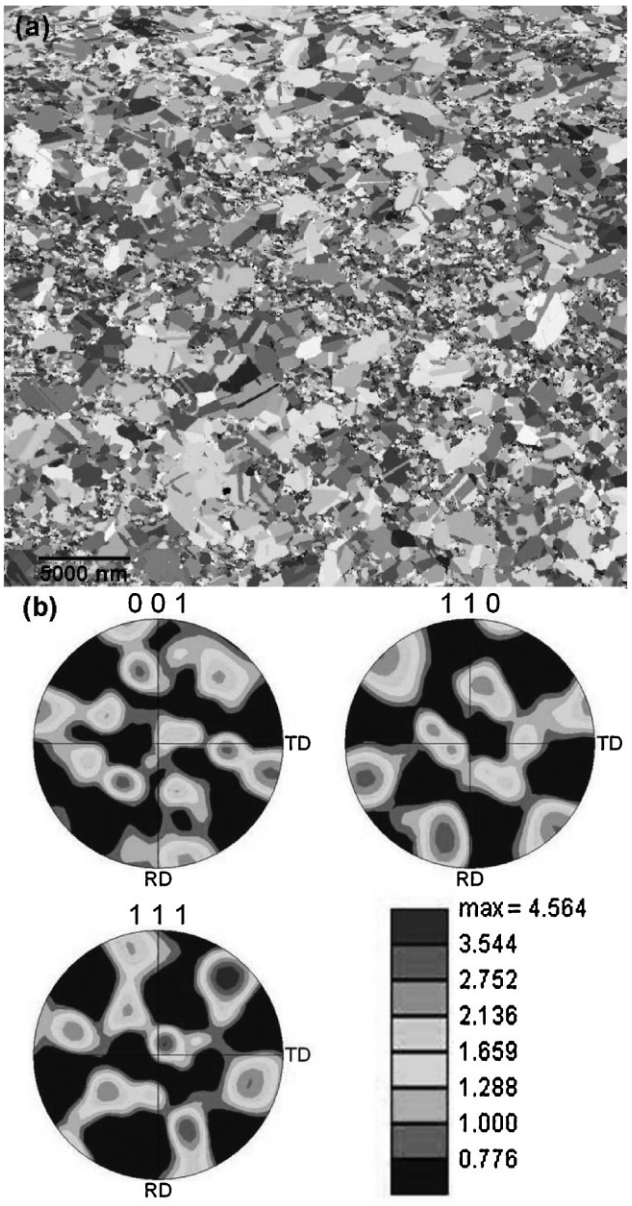

Fig. 4. (a) Representative EBSD image of the bimodal Cu sample annealed for 40 min. (b) (001), (101), and (111) pole figures in stereographic projection of the bimodal Cu sample, which exhibit ill-defined textures suggestive of a small sampling from a random texture.

Mechanical Property–Microstructure Relationship

Figure 6 shows the yield strength (a) and uniform elongation (b) versus the volume fraction of recrystallized micro-grains. The yield strength decreases, while the uniform elongation increases with increasing X_V, and both have an approximately linear relationship with X_V suggesting a rule-of-mixtures relationship.[23] To test the validity of this hypothesis, we used the following rule-of-mixtures equations to calculate the yield strength σ and uniform elongations ε:

$$\sigma = (1-X_V)\sigma_{UFG} + X_{V\sigma CG} \quad (2)$$

$$\varepsilon = (1-X_V)\varepsilon_{UFG} + X_V\varepsilon_{CG} \quad (3)$$

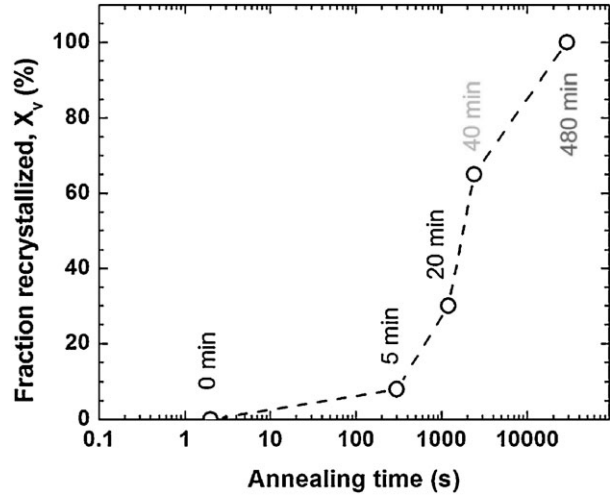

Fig. 5. Volume fraction of recrystallized macro-grain region X_V of the bimodal Cu sample against the annealing time.

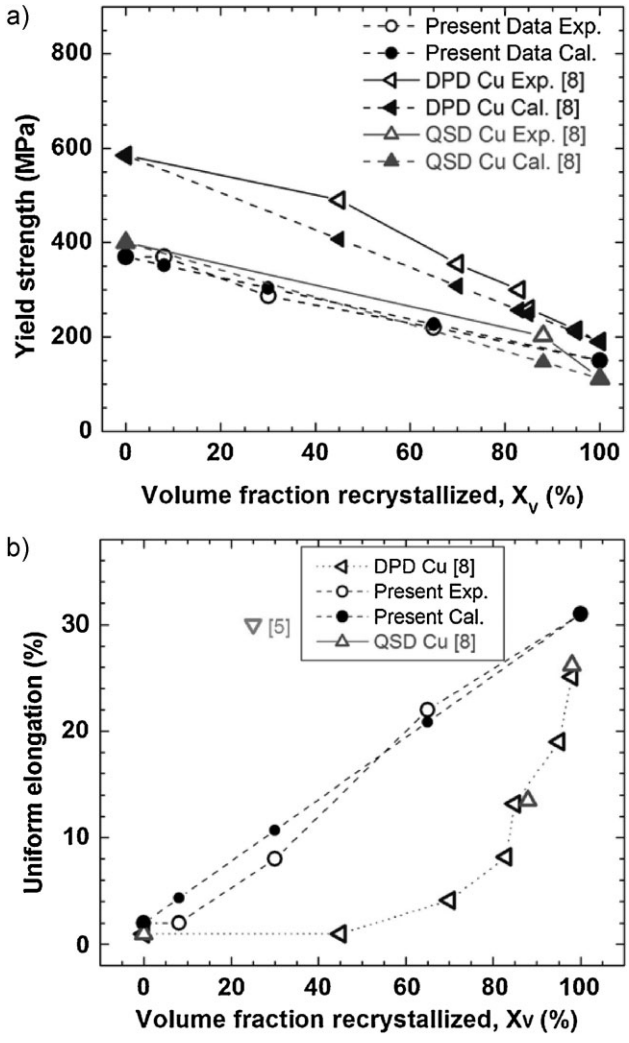

Fig. 6. Experimental and calculated yield strength (a) and uniform elongation (b) versus the volume fraction of recrystallized, X_V, from present results and the bi-modal Cu prepared by DPD and QSD.[8]

where σ_{UFG} and σ_{CG} are the yield strengths of the UFG matrix and micro-grains, and equal 370 (0 min, $X_V = 0$) and 150 MPa (480 min, $X_V = 100\%$), respectively. ε_{UFG} and ε_{CG} are the uniform elongation values of the UFG matrix and micro-grains, and equal 2 (0 min, $X_V = 0$) and 26% (480 min, $X_V = 100\%$), respectively. The calculated yield strength and uniform elongation (solid circles) based on the rule-of-mixtures versus X_V are compared with the experimental results (open circles) in Figure 6(a) and (b), respectively. The experimentally determined yield strength and uniform elongation values are consistent with those predicted on Equations 2 and 3. In addition, yield strength values obtained from the literature[8] were also calculated (solid triangles) and compared with experimental results (empty triangles) in Figure 4(a), and appear to be consistent with the approximate rule-of-mixtures approximation.

In related studies, Raeisinia *et al*.[35] used a micromechanics polycrystalline model to simulate the monotonic plastic deformation of polycrystal Cu with a bimodal grain size distribution, and found the variations of both ultimate tensile strength and uniform elongation against X_V follow the rule-of-mixtures approximation. By incorporating 3 μm grains to the 200 nm grain matrix, Raeisinia *et al*. found that the uniform elongation of the bimodal materials is gradually restored at the expense of the strength.[35] The uniform elongation exhibits an approximately linear relationship with the X_V, following the rule-of-mixtures prediction. Moreover, the ultimate tensile strength of the bimodal materials decreased approximately linearly with increasing X_V also following the rule-of-mixtures. In addition, Joshi *et al*.[36] modeled the mechanical response of 5083 Al alloy with a bimodal grain size distribution by using the secant Mori–Tanaka (M-T) mean-field approach, and also reported that the ultimate tensile stress and uniform elongation follow a rule-of-mixtures prediction.

The uniform elongation values obtained from the literature[5,8] were compared in Figure 6(b). In addition to the two contradictory trends of positive and negative deviations from the rule-of-mixtures, as discussed in the introduction part, our present result revealed a third case which is consistent with a rule-of-mixtures prediction. These differences in the relationship between uniform elongation an X_V may be attributed to differences in microstructural characteristics, such as different spatial distributions of the UFG and CG grains, and or possibly different size differences between the micro-grains and the UFG matrix. The UFG microstructure of our as-ECAP sample is uniform due to large deformation strain of 16 passes of Bc route, and this results in the uniform and random distribution of the recrystallized micro-grains among UFG matrix, as revealed by Figure 3 and 4. However, the nanocrystalline Cu prepared by DPD[8] consisted of ≈33 vol% nanoscale twin bundles embedded in 80 nm nanograins, and recrystallization occurred selectively in regions of the microstructure that did not contain twin bundles. This resulted in the formation of micro-grain agglomerates that were heterogeneously distributed throughout the nanocrystalline matrix.[8] Moreover, the size difference between the UFG and micro-grains of the present bi-modal Cu is much smaller than that corresponding to the results presented in ref. [8. The micro-grains are about 1–3 μm and the UFG matrix is about 300 nm in the present bimodal Cu. However, in published studies,[8] the micro-grains are about 1–6 μm, and the UFG is 73 nm. Accordingly, we propose that both factors, that is the presence of a heterogeneous spatial distribution of grains and a large size difference between micro- and UFG-grains, will lead to heterogeneous plastic deformation and associated stress concentration, causing a premature necking instability, i.e., low ductility. The bimodal microstructure in ref. [5 is similar to that of the bimodal Cu studied herein. In this case, however, the observed positive deviation from the rule-of-mixtures prediction is not presently understood, and additional studies are underway to clarify the underlying mechanisms.

Conclusions

In summary, by using UFG Cu with homogeneous microstructures as initial modal materials and low-temperature oil-bath annealing, we successfully prepared bimodal Cu with homogeneous distribution of different-volume-fraction recrystallized micro-grains within the UFG matrix. Tensile results and microstructural analyses indicate that both yield strength and uniform elongation of the bimodal Cu follow the rule-of-mixtures. Our work provides a pathway for optimizing the mechanical properties of multi-scale materials with bimodal grain size distribution.

Received: January 21, 2011
Final Version: February 25, 2011
Published online: April 18, 2011

[1] C. C. Koch, D. G. Morris, K. Lu, A. Inoue, *MRS Bull.* **1999**, *24*, 54.
[2] Y. H. Zhao, Y. T. Zhu, E. J. Lavernia, *Adv. Eng. Mater.* **2010**, *12*, 769.
[3] M. Legros, B. R. Elliott, M. N. Rittner, J. R. Weertman, K. J. Hemker, *Philos. Mag. A* **2000**, *80*, 1017.
[4] V. L. Tellkamp, A. Melmed, E. J. Lavernia, *Metall. Mater. Trans. A* **2001**, *32*, 2335.
[5] Y. M. Wang, M. W. Chen, F. H. Zhou, E. Ma, *Nature* **2002**, *419*, 912.
[6] Y. H. Zhao, T. Topping, J. F. Bingert, J. J. Thornton, A. M. Dangelewicz, Y. Li, W. Liu, Y. T. Zhu, Y. Z. Zhou, E. J. Lavernia, *Adv. Mater.* **2008**, *20*, 3028.
[7] Y. H. Zhao, E. J. Lavernia, Mechanical properties of multi-scale metallic materials, in: *Nanostructured Metals and Alloys: Processing, Microstructure and Properties*, Woodhead Publishing, Cambridge, UK **2011**.
[8] Y. S. Li, Y. Zhang, N. R. Tao, K. Lu, *Scr. Mater.* **2008**, *89*, 475.

[9] T. Sano, G. S. Rohrer, *J. Am. Ceram. Soc.* **2007**, *90*, 211.
[10] Z. Lee, V. Radmilovic, B. Ahn, E. J. Lavernia, S. R. Nutt, *Metall. Mater. Trans. A* **2010**, *41*, 795.
[11] S. Billard, J. P. Fondere, B. Bacroix, G. F. Dirras, *Acta Mater.* **2006**, *54*, 411.
[12] H. Jin, D. J. Lloyd, *Scr. Mater.* **2004**, *50*, 1319.
[13] G. J. Fan, H. Choo, P. K. Liaw, E. J. Lavernia, *Acta Mater.* **2006**, *54*, 1759.
[14] B. Srinivasarao, K. Oh-ishi, T. Ohkubo, T. Mukai, K. Hono, *Scr. Mater.* **2008**, *58*, 759.
[15] H. Azizi-Alizamini, M. Militzer, W. J. Poole, *Scr. Mater.* **2007**, *57*, 1065.
[16] J. Gubicza, H. Q. Bui, F. Fellah, G. F. Dirras, *J. Mater. Res.* **2009**, *24*, 217.
[17] T. R. Lee, C. P. Chang, P. W. Kao, *Mater. Sci. Eng, A* **2005**, *408*, 131.
[18] D. Das, A. Samanta, P. P. Chattopadhyay, *Metal-Org. Nano-Metal Chem.* **2006**, *36*, 221.
[19] E. Rabkin, I. Gutman, M. Kazakevich, E. Buchman, D. Gorni, *Mater. Sci. Eng, A* **2005**, *396*, 11.
[20] C. X. Huang, S. D. Wu, G. Y. Li, S. X. Li, *Mater. Sci. Eng, A* **2008**, *483*, 433.
[21] M. C. Zhao, F. Yin, T. Hanamura, K. Nagai, A. Atrens, *Scr. Mater.* **2007**, *57*, 857.
[22] T. Niendorf, D. Canadinic, H. J. Maier, I. Karaman, *Scr. Mater.* **2009**, *60*, 344.
[23] V. Laws, *J. Mater. Sci. Lett.* **1983**, *2*, 527.
[24] J. G. Sevillano, J. Aldazabal, *Scr. Mater.* **2004**, *51*, 795.
[25] Y. H. Zhao, Y. Li, T. D. Topping, X. Z. Liao, Y. T. Zhu, R. Z. Valiev, E. J. Lavernia, *Int. J. Mater. Res.* **2009**, *100*, 1647.
[26] Y. H. Zhao, Y. Z. Guo, Q. Wei, A. M. Dangelewicz, C. Xu, Y. T. Zhu, T. G. Langdon, Y. Z. Zhou, E. J. Lavernia, *Scr. Mater.* **2008**, *59*, 627.
[27] Y. H. Zhao, Y. Z. Guo, Q. Wei, T. D. Topping, A. M. Dangelewicz, Y. T. Zhu, T. G. Langdon, E. J. Lavernia, *Mater. Sci. Eng, A* **2009**, *525*, 68.
[28] J. Y. Huang, Y. T. Zhu, H. Jiang, T. C. Lowe, *Acta Mater.* **2001**, *49*, 1497.
[29] R. Z. Valiev, R. K. Isamgaliev, I. V. Alexandrov, *Prog. Mater. Sci.* **2000**, *45*, 103.
[30] W. A. Johnson, R. F. Mehl, *Trans. Metall. Soc. AIME* **1939**, *135*, 416.
[31] R. A. Vandermeer, P. Gordon, *Trans. Metall. Soc. AIME* **1959**, *215*, 577.
[32] N. Hansen, B. Bay, *Acta Metall.* **1981**, *29*, 65.
[33] J. T. Michalak, W. R. Hibbard, *Trans. ASM* **1961**, *53*, 331.
[34] R. A. Vandermeer, B. B. Rath, *Metall. Trans. A* **1989**, *20*, 391.
[35] B. Raeisinia, C. W. Sinclair, W. J. Poole, C. N. Tome, *Modell. Simul. Mater. Sci. Eng.* **2008**, *16*, 025001.
[36] S. P. Joshi, K. T. Ramesh, B. Q. Han, E. J. Lavernia, *Metall. Mater. Trans. A* **2006**, *37*, 2397.

